

# Limb-Darkening Anomalies in Stars Eclipsed by Exoplanets

M. K. Abubekero\*, N. Yu. Gostev, and A. M. Cherepashchuk

*Sternberg Astronomical Institute, Moscow State University, Moscow, Russia*

Received March 26, 2014; in final form, June 9, 2014

**Abstract**—The possibility of explaining discrepancies between observed and theoretical limb-darkening coefficients as being a manifestation of the extended, non-spherical atmosphere of an eclipsing exoplanet is analyzed, assuming the model stellar atmospheres used are correct.

**DOI:** 10.1134/S1063772915010011

## 1. INTRODUCTION

A detailed analysis of high-accuracy, multi-color light curves of the binary system with an exoplanet HD 209458 [1] demonstrated a discrepancy between the observed limb-darkening coefficients and theoretical values obtained from model stellar atmospheres. A more detailed study of the differences between observational and theoretical limb-darkening coefficients for HD 209458 showed that this difference can not be avoided, even when a fairly wide range of parameters of the model stellar atmosphere is considered [2]. Claret [2] referred to HD 209458 as a “challenge to the theory of stellar atmospheres.” We attempted to identify a way of removing the discrepancy between the observed and theoretical limb-darkening coefficients in our earlier paper [3], where we showed that even the use of confidence intervals to estimate the “external” errors is not able to remove this discrepancy. †

It is possible that the discrepancy is due to the use of a model that is too simple. For example, a model with two spherical stars is not able to fully take into account the interaction between a star and its planet.

The importance of taking into account the effects of the interaction between the star and exoplanet has been confirmed by new observational data. For example, analysis of a transit near-UV light curve of the binary with an exoplanet WASP-12b showed a much deeper and wider eclipse compared to the photometric transit light curve in the visible [4]. This suggests deformation of the planetary magnetosphere and atmosphere under the action of the stellar wind [5, 6]. The WASP-12b system is composed of a late  $1.35 M_{\odot}$  star with a surface temperature of 6300 K and a  $1.4 M_J$  exoplanet located at a distance of 0.0229 AU ( $M_J$  is the mass of Jupiter). The orbital period of

the system is  $1.09^d$ . These parameters are fairly close to the parameters of binaries we have studied—HD 209458 and HD 189733. The possible deformation of the magnetosphere and atmosphere of exoplanets due to the stellar winds of their central stars is also confirmed by three-dimensional gas-dynamical modeling of the behavior of the atmosphere of the hot Jupiter in WASP-12b, which is located close to its star [7]. The WASP-12b system resembles the binary systems HD 209458 and HD 189733.

The results of the 3D gas-dynamical modeling [7, 8] indicate that the atmosphere of the exoplanet HD 209458b is perturbed by the stellar wind. Due to the comparatively high temperature of the planetary atmosphere, the outflow of matter from its surface is sufficiently strong for the planet to acquire a cometary tail [9, 10]. One of the reasons for this strong disturbance by the stellar wind of the central star is the weakness of the exoplanet’s magnetic field, which is unable to withstand the stellar wind.

Our previous studies [3, 11–14] treated the planet like a spherical body with a sharp edge. The new analyses of [4, 10] suggest that this idealized model is oversimplified. We thus cannot rule out that the discrepancy between the observed and theoretical limb-darkening coefficients of HD 209458 and HD 189733 is due to the application of model for the explanet atmospheres that is too idealized, rather than inadequacy of current models for thin stellar atmospheres.

To investigate this question, we fixed the limb-darkening coefficients when fitting the eclipse data for HD 209458 and HD 189733 in our current study. We used values yielded by the latest theoretical computations of Claret [15] obtained using PHOENIX model for the limb-darkening coefficients of HD 209458 and HD 189733. Assuming spherical model components moving in circular orbits, we searched for the orbital inclination  $i$ , relative radius of the exoplanet  $r_p$ , and

\*E-mail: marat.abubekero@gmail.com

**Table 1.** Results of fitting the observed light curves of HD 209458 [16], using a quadratic limb-darkening law with fixed coefficients (errors are  $1\sigma$ , and were estimated using the differential-corrections method; the two rightmost columns list the reduced  $\chi^2$  and corresponding significance levels  $\alpha$ )

$\lambda, \text{\AA}$	$r_s$	$\sigma(r_s)$	$r_p$	$\sigma(r_p)$	$r_p/r_s$	$\sigma(r_p/r_s)$	$i$	$\sigma(i)$	$\chi_{\text{red}}^2$	$\alpha$
3201	0.1131	0.00053	0.01385	0.000062	0.12239	0.0046	86.71°	0.035	1.07	0.16
3750	0.1102	0.00028	0.01323	0.000030	0.12003	0.0026	87.17	0.022	1.10	0.07
4300	0.1112	0.00018	0.01335	0.000019	0.12003	0.0016	87.04	0.013	1.19	0.00
4849	0.1109	0.00016	0.01326	0.000018	0.11958	0.0014	87.11	0.013	1.30	0.00
5398	0.1117	0.00016	0.01341	0.000018	0.12005	0.0014	87.00	0.013	1.20	0.00
5802	0.1122	0.00015	0.01356	0.000016	0.12092	0.0013	86.89	0.012	1.46	0.00
6779	0.1123	0.00014	0.01350	0.000015	0.12019	0.0012	86.89	0.012	1.46	0.00
7755	0.1112	0.00016	0.01336	0.000019	0.12010	0.0014	86.98	0.015	1.32	0.00
8732	0.1119	0.00020	0.01347	0.000024	0.12043	0.0018	86.91	0.018	1.20	0.00
9708	0.1107	0.00030	0.01339	0.000035	0.12096	0.0027	87.04	0.028	1.23	0.00

The closeness of  $\alpha$  to 0 is related to the fixed coefficients in the quadratic limb-darkening law.

relative radius of the star  $r_s$  as a function of the wavelength  $\lambda$ . The parameters  $i$  and, to an appreciable extent,  $r_s$  should not depend on the wavelength. At the same time, if the exoplanet has a significant atmosphere, the radius  $r_p$  may depend substantially on  $\lambda$ . If a wavelength dependence is also found for both  $i$  and  $r_s$ , this implies inadequacy of the model used to describe the eclipsing binary, due to failure to take into account the exoplanet atmosphere, its cometary tail, and so on.

## 2. OBSERVATIONAL DATA AND FITTING

We consider here the observed light curves of the binary systems HD 209458 and HD 189733, which have similar parameters. Despite this similarity, HD 189733 displays a satisfactory agreement between the observed and theoretical limb-darkening coefficients, while HD 209458 does not.

As observational material for HD 209458, we used multi-color light curves obtained with the Hubble Space Telescope (HST) from May 3 to July 6, 2003 [16]. The central wavelengths of these transit light curves are  $\lambda = 3201, 3750, 4300, 4849, 5398, 5802, 6779, 7755, 8732, \text{ and } 9708 \text{ \AA}$ . Each light curve includes  $\sim 500$  individual brightness measurements for HD 209458. The rms error of the individual measurements varies from  $1.79 \times 10^{-4}$  to  $6.09 \times 10^{-4}$  (from  $\sim 10^{-2}$  to  $\sim 3 \times 10^{-2}$  relative to the depth of the eclipse). More detailed information on these observational data and their reduction is provided in [16]. The observed transit light curves for HD 209458 are presented in Fig. 1.

As observational material for HD 189733, we used multi-color light curves obtained with the HST on May 22, May 26, and July 14, 2006 [17]. Ten light curves of eclipses in the ranges  $\lambda = 5500\text{--}6000, 6000\text{--}6500, 6500\text{--}7000, 7000\text{--}7500, 7500\text{--}8000, 8000\text{--}8500, 8500\text{--}9000, 9000\text{--}9500, 9500\text{--}10\,000, 10\,000\text{--}10\,500 \text{ \AA}$  were obtained. More detailed information on these observational data can be found in [17]. In our analyses of these light curves, we adopted the central wavelengths  $\lambda = 5750, 6250, 6750, 7250, 7750, 8250, 8750, 9250, 9750, \text{ and } 10\,250 \text{ \AA}$ . Each light curve contains 675 individual brightness measurements with uncertainties  $\sim 5 \times 10^{-4}$  of the normalized out-of-eclipse brightness. The observed transit light curves of HD 189733 are presented in Fig. 2.

We fitted the transit light curves using a model with a spherical star eclipsed by a spherical exoplanet (the classical problem with two spherical stars), without taking into account the effects of the proximity of the two components. Such a model can easily be computed on modern computers, making it possible to solve a large number of model versions using a relatively small amount of computer time [11]. The model and algorithm used to fit the transit light curves are described in more detail in [3, 11–14].

Since the transit light curve of HD 189733 displays a disturbance due to the spottedness of the stellar surface [18] close to the minimum and on the right branch (Fig. 2), only the left branch of the light curve, up to orbital phase  $178^\circ$ , was fitted. It was shown in [13] that the left branch of the light curve is

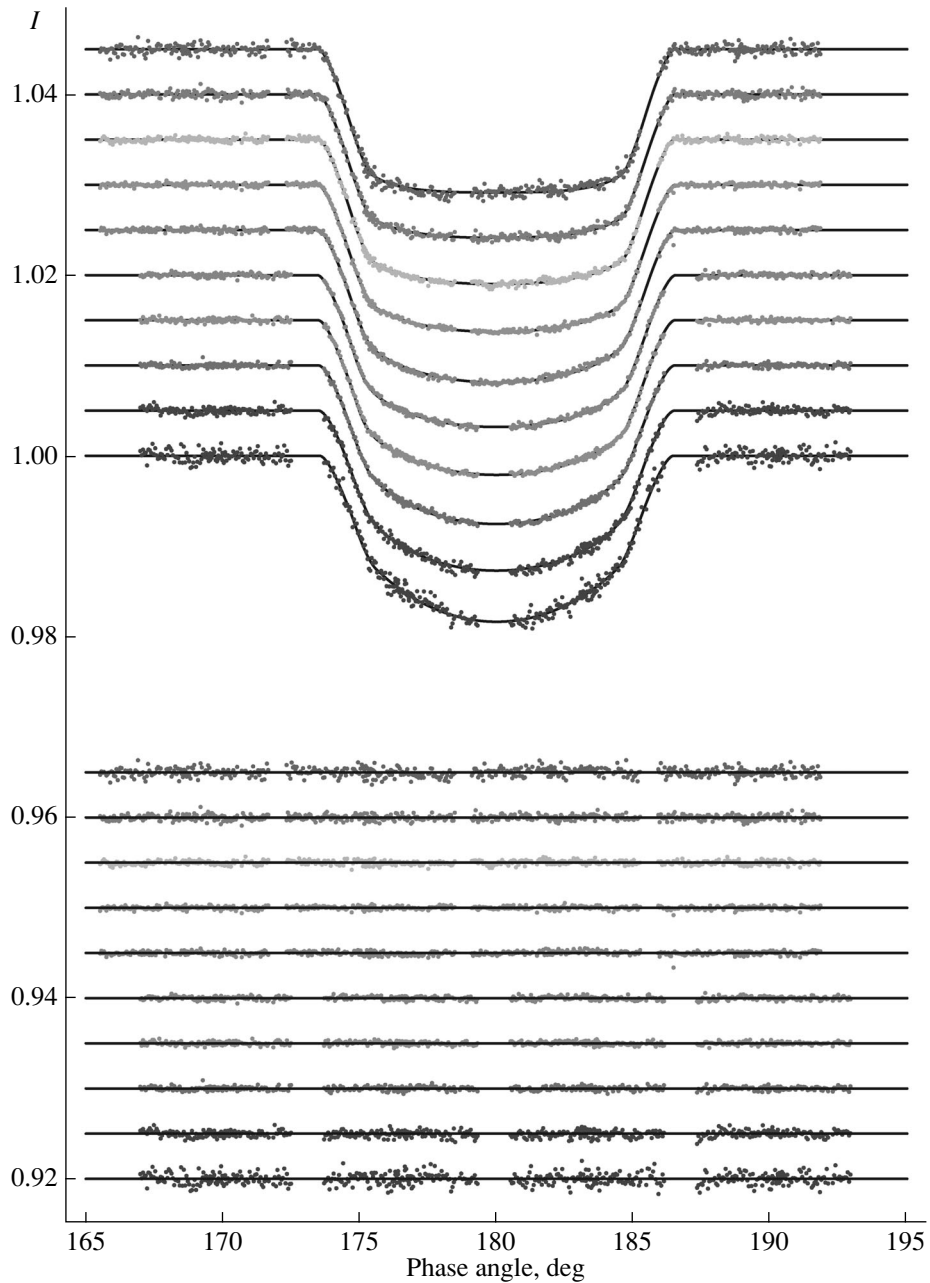


**Fig. 1.** Observed light curves of HD 209458 [16] constructed for wavelengths 3201, 3750 4300, 4849 5398, 5802, 6779, 7755, 8732, and 9708 Å (upper set of curves, with the wavelength increasing upward). The lower set of curves show the corresponding residuals. The solid curves show theoretical curves obtained for the model with a nonlinear (quadratic) limb-darkening law and the fixed coefficients from [15].

most reliable for the observational data we are using here.

### 3. RESULTS

The results of our fitting of the transit light curves of HD 209458 are presented in Table 1, and are shown graphically in Figs. 3–6. The results of our fitting of the transit light curves of HD 189733 are presented in Table 2 and Figs. 7–10.

As can be seen from Table 1, the critical significance levels  $\alpha$  for the models derived from the transit light curves of HD 209458 with  $\lambda \geq 4300$  Å are close to zero. Thus, these models fit the observational data relatively poorly. This is most probably due to the fact that the limb-darkening coefficients were fixed. Note that this also affects the wavelength dependences of the derived parameters. The dependences presented

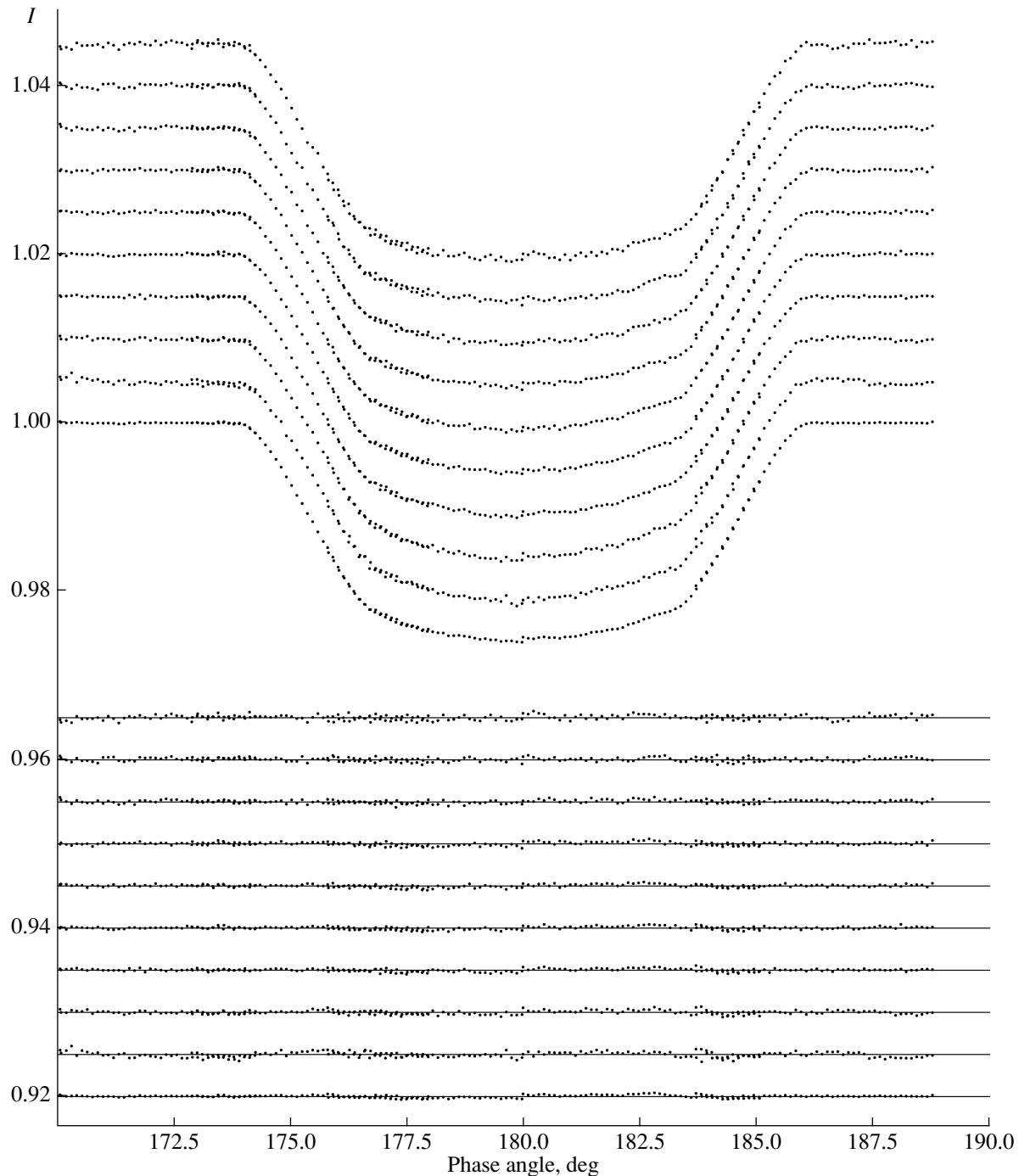


**Fig. 2.** Observed light curves of HD 189733 at  $\lambda = 5500\text{--}10\,500$  (upper set of curves, with the wavelength increasing upward). The lower set of curves shows the residuals for a quadratic limb-darkening law for the best-fit values of the parameters and the fixed darkening coefficients from [15].

in Figs. 3–6 show that the points are generally scattered irregularly.

The spherical model [3] satisfies the observational data for HD 189733 significantly better. The wavelength dependences of the parameters shown in Figs. 7–10 are more regular, and we can distinguish a single trend in each case. Since the model derived

using the light curve for the central wavelength  $\lambda = 5750\text{ \AA}$  is rejected by the  $\chi^2_{\text{red}}$  criterion, the parameters obtained from this light curve were not used in our overall analysis.

We used linear fits and their rms values to find and analyze the wavelength dependences of the orbital

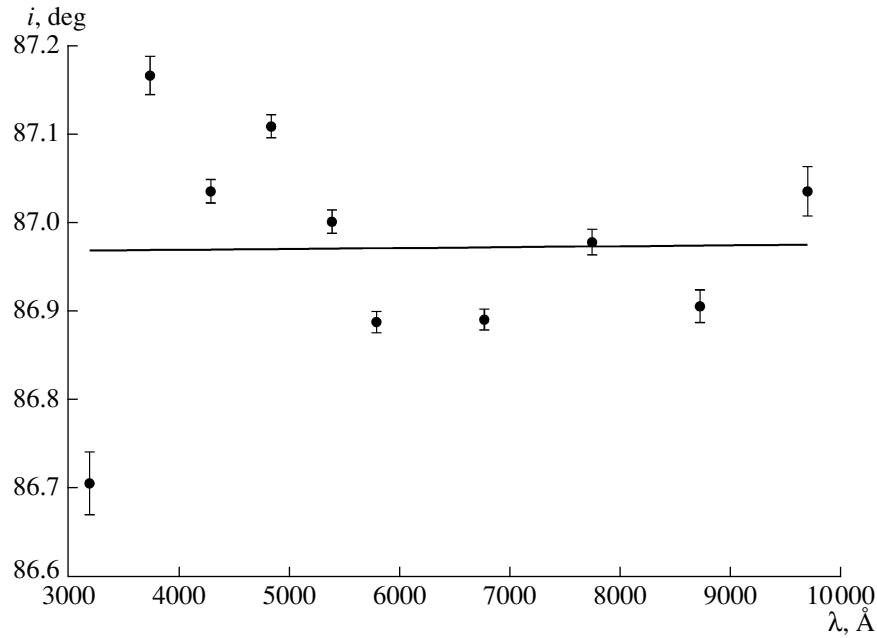


**Fig. 3.** Dependence of  $i$  on the photometric wavelength, obtained for HD 209458 by fitting the transit light curves using a quadratic limb-darkening law with the fixed coefficients [15]. The solid line shows the least-squares fit.

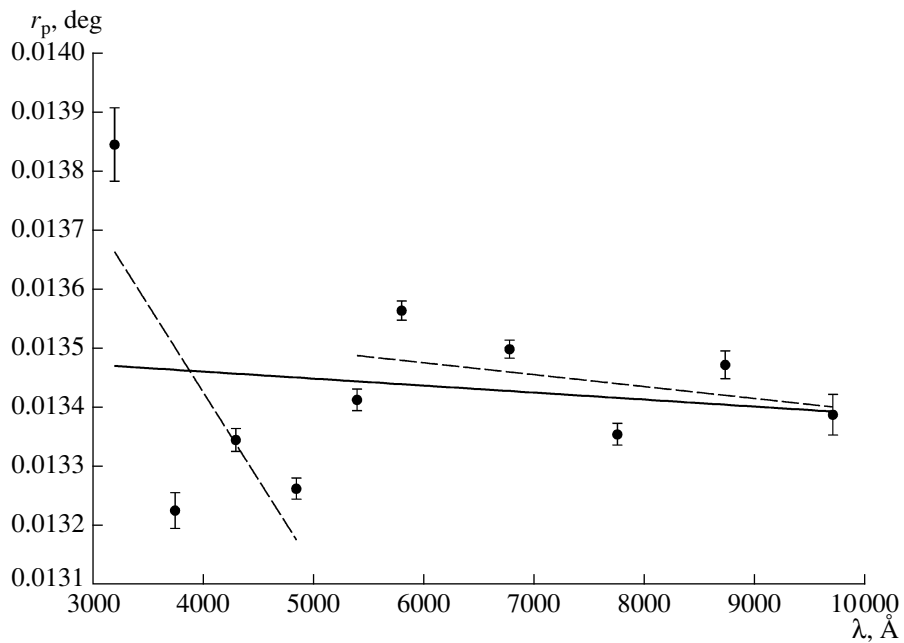


**Fig. 4.** Dependence of  $r_p$  on the photometric wavelength, obtained for HD 209458 by fitting the transit light curves using a quadratic limb-darkening law with the fixed coefficients [15]. The solid line shows the dependence obtained for the entire range  $\lambda = 3201\text{--}9708$  Å, while the dashed lines show the least-squares fits for  $\lambda < 5000$  Å and  $\lambda > 5000$  Å.

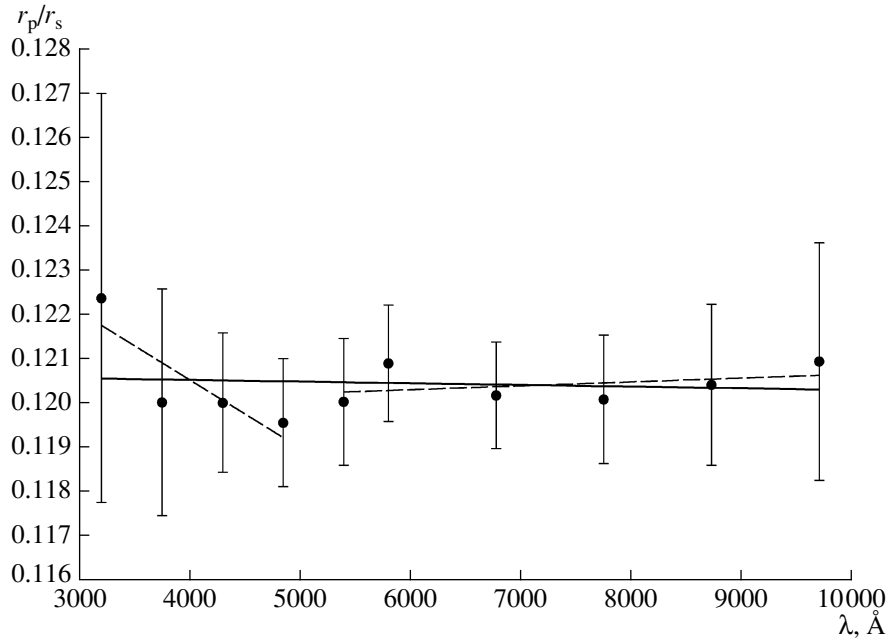


Fig. 5. Same as Fig. 4 for the ratio  $r_p/r_s$ .

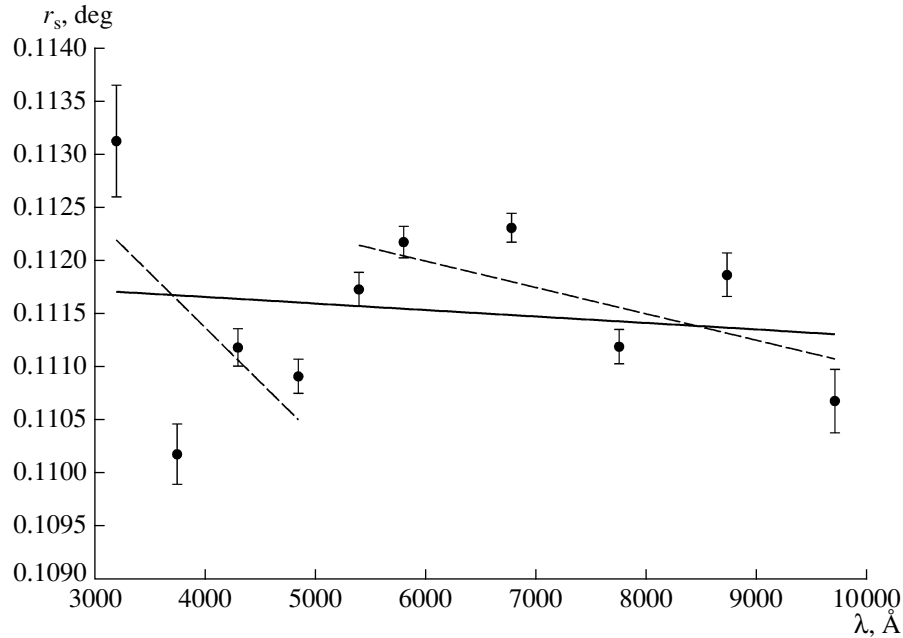


Fig. 6. Same as Fig. 4 for  $r_s$ .

inclination  $i$ , exoplanet radius  $r_p$ , and stellar radius  $r_s$  for HD 209458 and HD 189733.

## 4. DISCUSSION

### 4.1. HD 209458

For HD 209458, we note only a weak dependence of  $i$  on  $\lambda$  (Fig. 3). The dependences of  $r_p$ ,  $r_s$ , and  $r_p/r_s$

on  $\lambda$  are more pronounced, although the scatter of the points on the corresponding trend is fairly large.

Figure 4 shows that the scatter of points relative to the trend indicated by the rms deviations about the linear fit is fairly large. Deviations from the trend are particularly large for  $\lambda < 5000$  Å. This led us to analyze the trends for the dependence of  $r_p$  on  $\lambda$

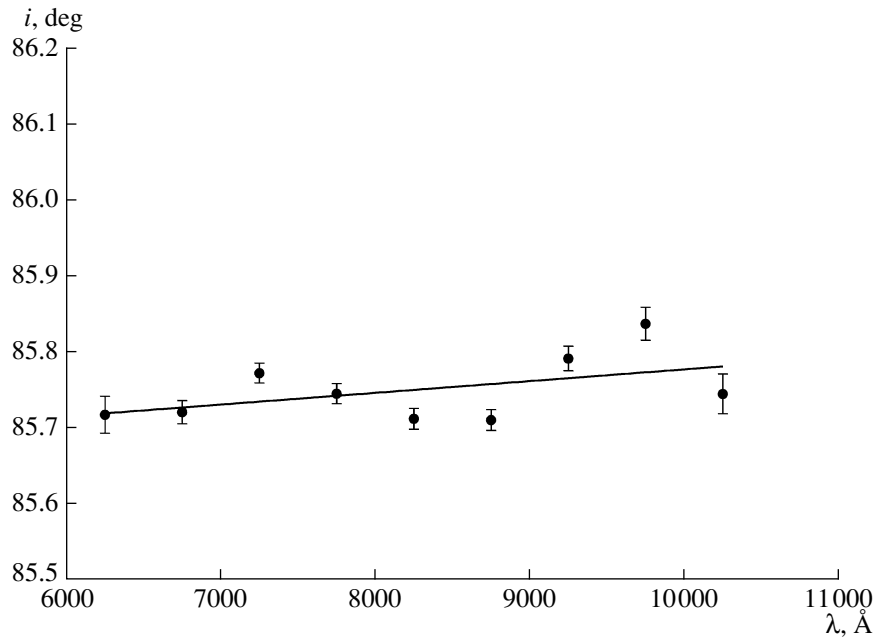


Fig. 7. Same as Fig. 3 for HD 189733.

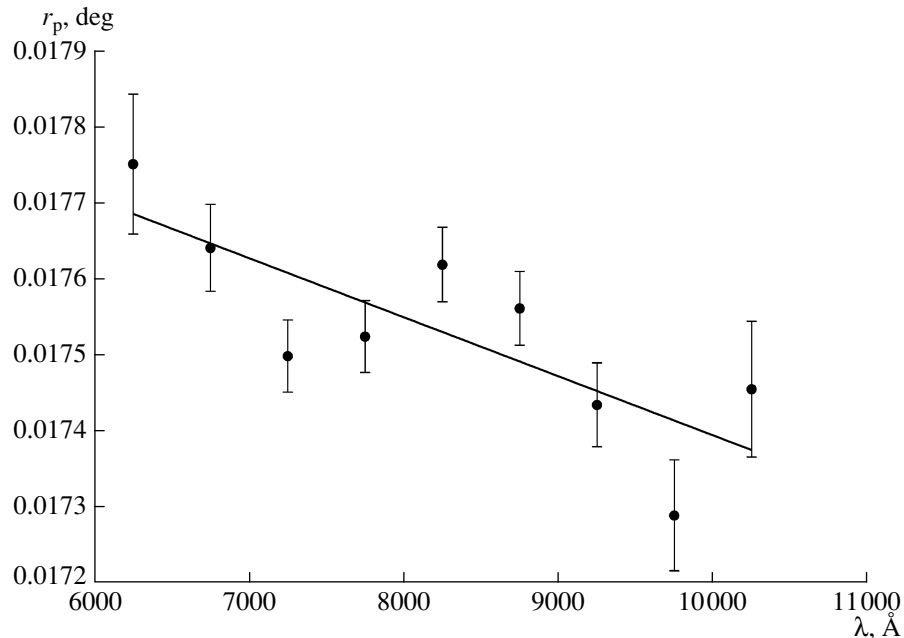


Fig. 8. Dependence of  $r_p$  on the photometric wavelength, obtained for HD 189733 using a quadratic limb-darkening law with the fixed coefficients [15]. The solid line shows the least-squares fit.

separately in the range  $\lambda < 5000 \text{ \AA}$  and  $\lambda > 5000 \text{ \AA}$  (Fig. 4). We proceeded in the same way in our analysis of the ratio of the exoplanet and stellar radii  $r_p/r_s$  and the stellar radius  $r_s$  (Figs. 5 and 6). The wavelength dependence of the exoplanet radius  $r_p$  for HD 209458b is stronger for  $\lambda < 5000 \text{ \AA}$  than for  $\lambda >$

$5000 \text{ \AA}$  (Fig. 4), although the dependence changes its sign if the point corresponding to  $\lambda = 3201 \text{ \AA}$  is not included.

The noted regions in Fig. 4 differ qualitatively in the mean slopes of the fitted lines. As expected, the dependence is steeper for  $\lambda < 5000 \text{ \AA}$  than for  $\lambda > 5000 \text{ \AA}$  (Fig. 4). This break confirms that the effects

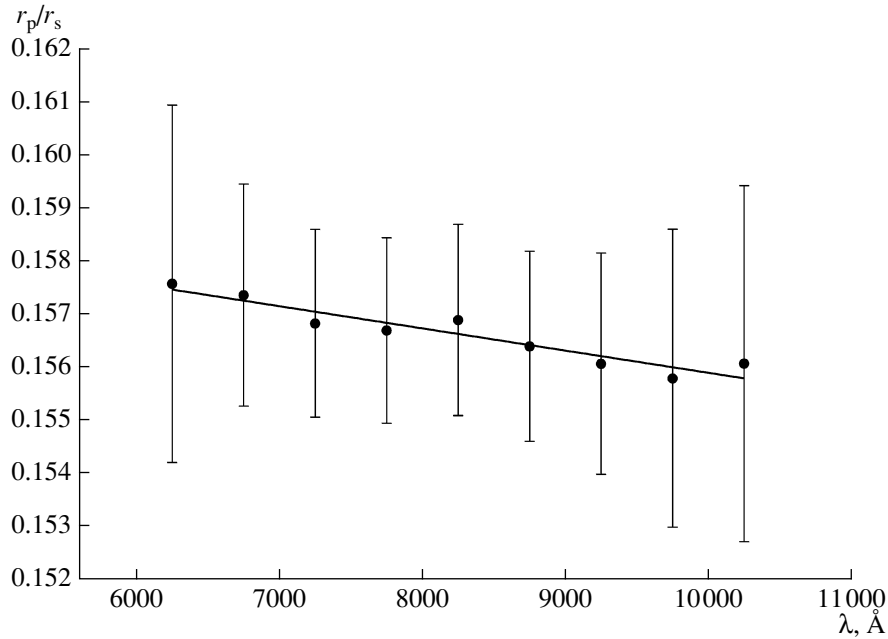


Fig. 9. Same as Fig. 8 for the ratio  $r_p/r_s$ .

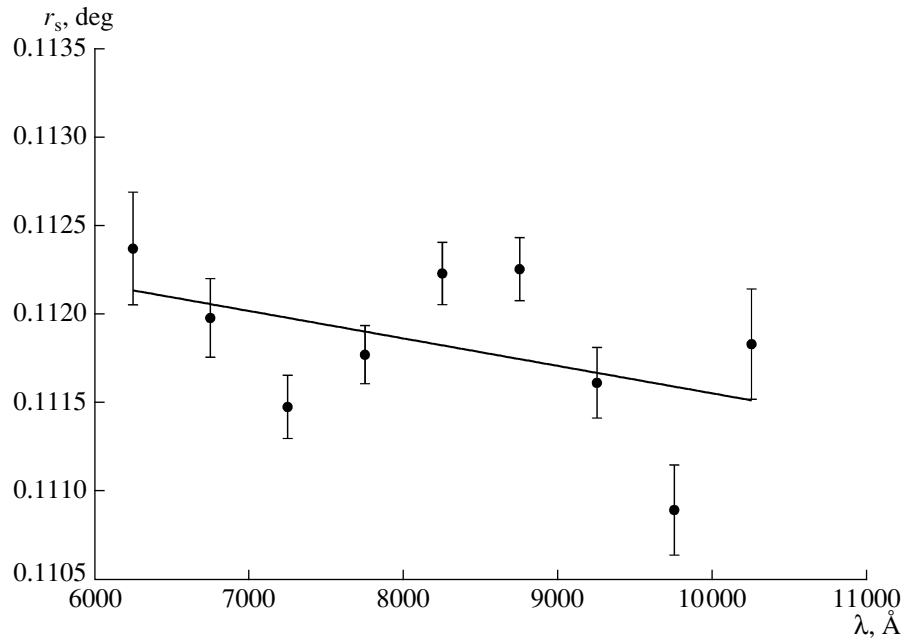


Fig. 10. Same as Fig. 8 for  $r_s$ .

of absorption by the distorted exoplanet atmosphere are important in the blue part of the spectrum.

According to the recent studies [7, 8], due to its weak magnetic field and interaction with the stellar wind from its central star, the hot Jupiter in the HD 209458b system is significantly non-spherical, and has a gas plume similar to a cometary tail. Thus,

the dependence shown in Fig. 4 fits the picture of the exoplanet HD 209458b as a cometary planet [7, 8].

Our conclusions concerning HD 209458 are in qualitative agreement with the conclusions derived by Fossatti et al. [4], who showed that the WASP-12b transit light curve in the UV differs significantly from the visual light curve, in terms of both its duration and the depth of the eclipse.

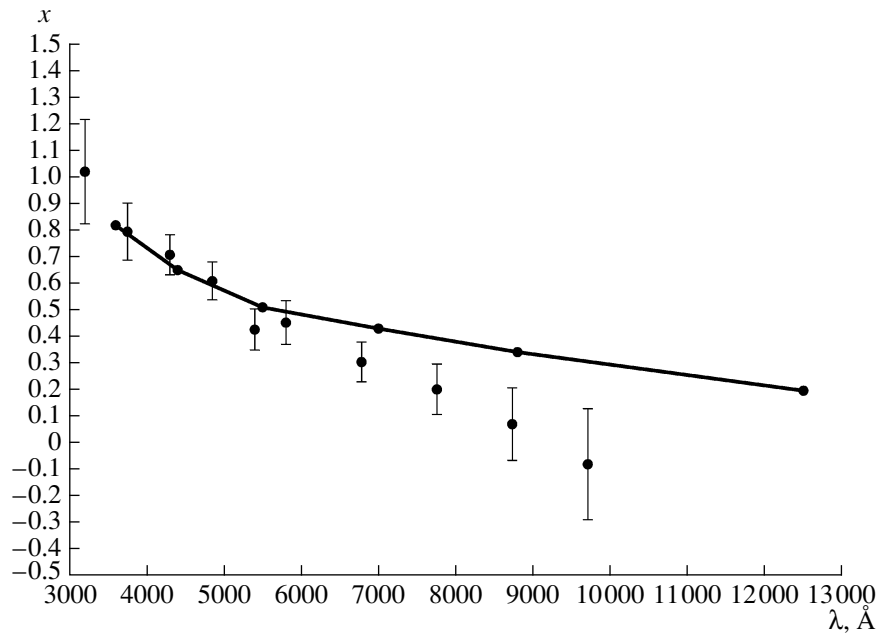


**Fig. 11.** Dependence of the observational [12] and theoretical [15] linear coefficient of the quadratic limb-darkening law for HD 209458 on the central photometric wavelength. The uncertainties in the limb-darkening coefficient  $x$  were obtained using the differential-corrections method. The errors shown are  $1\sigma$ .

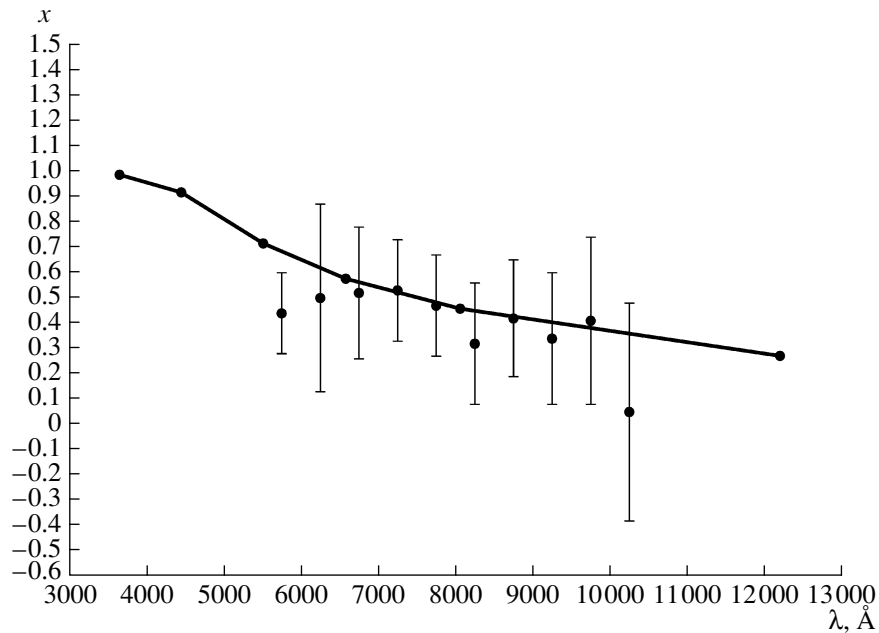


**Fig. 12.** Dependence of the observational [13] and theoretical [15] linear coefficients of the quadratic limb-darkening law for HD 189733 on the central photometric wavelengths. The uncertainties in the limb-darkening coefficient  $x$  were obtained using the differential-corrections method. The errors shown are  $1\sigma$ .

This suggests that the absorption in the visual at  $\lambda > 5000 \text{ \AA}$  is lower than in the UV, so that the slope of the line representing the trend for  $\lambda > 5000 \text{ \AA}$  in Fig. 4 is appreciably different from the slope for

$\lambda < 5000 \text{ \AA}$ . The wavelength dependence of the exoplanet radius becomes less pronounced at  $\lambda > 5000 \text{ \AA}$  (Fig. 4).

For completeness, Fig. 11 shows the wavelength dependence of the observational values of the linear

**Table 2.** Results of fitting the observed light curves (left branch) of HD 189733 [18]. For remaining comments on the table, see Table 1.

$\lambda, \text{\AA}$	$r_s$	$\sigma(r_s)$	$r_p$	$\sigma(r_p)$	$r_p/r_s$	$\sigma(r_p/r_s)$	$i$	$\sigma(i)$	$\chi_{\text{red}}^2$	$\alpha$
5750	0.1102	0.00028	0.01717	0.000061	0.1558	0.0025	86.03°	0.018	5.56	0.00
6250	0.1127	0.00039	0.01775	0.000092	0.1576	0.0034	85.72	0.024	0.58	1.00
6750	0.1121	0.00024	0.01764	0.000057	0.1574	0.0021	85.72	0.015	0.52	1.00
7250	0.1116	0.00020	0.01750	0.000048	0.1568	0.0018	85.77	0.013	0.69	0.98
7750	0.1118	0.00020	0.01752	0.000047	0.1567	0.0017	85.75	0.013	1.02	0.55
8250	0.1123	0.00021	0.01762	0.000049	0.1569	0.0018	85.71	0.014	1.80	0.0005
8750	0.1123	0.00021	0.01756	0.000049	0.1564	0.0018	85.71	0.014	0.88	0.81
9250	0.1117	0.00024	0.01743	0.000055	0.1561	0.0021	85.79	0.016	0.99	0.61
9750	0.1110	0.00032	0.01729	0.000073	0.1558	0.0028	85.84	0.022	1.38	0.054
10 250	0.1118	0.00038	0.01746	0.000090	0.1561	0.0034	85.75	0.026	0.62	1.00

Values  $\chi_{\text{red}}^2 < 1$  may indicate correlations between the data points on the light curves.

coefficient  $x$  of the quadratic limb-darkening law obtained earlier in [12]. This figure also shows the latest theoretical values for the limb-darkening coefficients obtained by Claret [15]. Figure 11 shows that the theoretical and observational values are in agreement for short wavelengths ( $\lambda < 5000 \text{ \AA}$ ), but disagree at  $\lambda > 5000 \text{ \AA}$ .

This all leads us to conclude that, although the long-wavelength range  $\lambda > 5000 \text{ \AA}$  is less affected by absorption by the extended atmosphere of the exoplanet in the case of HD 209458 (including the cometary tail), the observational values of the linear darkening coefficient in the quadratic law do not agree with the theoretical values for  $\lambda > 5000 \text{ \AA}$ . The reason for this discrepancy remains unclear.

#### 4.2. HD 189733

In the case of HD 189733, the model with two spherical bodies adequately describes the observed transit light curves according to the  $\chi^2$  criterion (apart from the transit light curve with the central wavelength  $\lambda = 5750 \text{ \AA}$ , which was not included in our analysis of the results of the fitting).

Orbital inclination of HD 189733 depends on the wavelength only weakly (Fig. 7). Unlike the exoplanet in the HD 209458 system, the wavelength dependence of the radius of the HD 209458 exoplanet is more regular. The radius of the exoplanet  $r_p$  varies by  $\sim 2.5\%$  at wavelengths  $\lambda = 6000\text{--}10\,000 \text{ \AA}$ , with  $r_p$  monotonically decreasing with increasing wavelength, providing evidence for the presence of an exoplanet atmosphere that scatters the stellar radiation

according to a Rayleigh law. The fact that the stellar radius  $r_s$  varies only slightly in this wavelength range (by  $\sim 0.7\%$ , see Fig. 10), suggests that the dependence of  $r_p$  on  $\lambda$  we have found is fairly reliable. This dependence confirms the action of Rayleigh scattering in the exoplanet atmosphere [13, 17].

We carried out a comparative analysis of the previously obtained linear limb-darkening coefficients in the quadratic law  $x$  [13] with the latest theoretical limb-darkening coefficients computed by Claret [15]. The observational and theoretical limb-darkening coefficients are in good agreement for HD 189733 (see Fig. 12), apart from the limb-darkening coefficient  $x$  based on the transit light curve for  $\lambda = 5750 \text{ \AA}$ , for which the model was rejected by the  $\chi_{\text{red}}^2$  criterion (Table 2).

## 5. CONCLUSION

We have analyzed multi-color transit light curves of the star–exoplanet binary systems HD 209458 and HD 189733 using the theoretical limb-darkening coefficients of [15] and a quadratic limb-darkening law. Supposing the model for the stellar atmosphere to be correct, we have checked whether the discrepancy between the observational [3, 11–14] and theoretical [2, 15] limb-darkening coefficients can be explained by the influence of an extended, non-spherical atmosphere around the exoplanet. In the case of HD 209458, the wavelength dependence of  $i$ ,  $r_s$ , and  $r_p$  is most significant at short wavelengths,  $\lambda = 3201\text{--}5000 \text{ \AA}$ , while these dependences are weaker at long wavelengths,  $\lambda = 5000\text{--}9708 \text{ \AA}$ . This most

likely indicates that the effects of the absorption of the stellar radiation by an extended, distorted atmosphere of the exoplanet are manifest at short wavelengths only, and are small at the longer wavelengths.

In this connection, it would seem that the observational values of the limb-darkening coefficients should be most different from the theoretical values at short wavelengths  $\lambda = 3201\text{--}5000 \text{ \AA}$  [2, 15]. However, the situation is the opposite in the case of HD 209458: there is good agreement of the observational and theoretical limb-darkening coefficient at short wavelengths (Fig. 11), while a significant discrepancy is observed at longer wavelengths. The reason for this discrepancy is unclear, leading us to acknowledge that HD 209458 remains a “challenge for the theory of stellar atmospheres,” as claimed by Claret [2].

In the case of HD 189733, the wavelength dependence of  $i$  is weak, and the relative variation of the stellar radius  $r_s$  with wavelength is less than  $\sim 1\%$ , indicating that the effects of absorption of the stellar radiation by a distorted, extended exoplanet atmosphere are insignificant at long wavelengths,  $\lambda = 6000\text{--}10\,000 \text{ \AA}$ , and a simple model for the binary system with two spherical bodies in circular orbits provides an adequate description of the available observational data. However, since the radius of the eclipsing exoplanet decreases with increasing wavelength by  $\sim 2.5\%$  at  $\lambda = 6000\text{--}10\,000 \text{ \AA}$ , this suggests that the exoplanet does have a quasi-atmosphere that scatters light according to a Rayleigh law. The observational limb-darkening coefficients [13] in the quadratic limb-darkening law are consistent with the theoretical values [2, 15] in the range  $\lambda = 6000\text{--}10\,000 \text{ \AA}$  in the case of HD 189733, confirming the validity of the modern theory of thin stellar atmospheres [15].

Further careful study of limb darkening in stars eclipsed by exoplanets are of considerable interest.

#### ACKNOWLEDGMENTS

This work was supported by a grant of the President of the Russian Federation for the State Support of Young Russian Phd Scientists (MK-893.2012.2) and the Russian Foundation for Basic Research (project 12-02-31466).

#### REFERENCES

1. J. Southworth, *Mon. Not. R. Astron. Soc.* **386**, 1644 (2008).
2. A. Claret, *Astron. Astrophys.* **506**, 1335 (2009).
3. M. K. Abubekkerov, N. Yu. Gostev, and A. M. Cherepashchuk, *Astron. Rep.* **52**, 99 (2008).
4. L. Fossati, C. A. Haswell, C. S. Froning, L. Hebb, S. Holmes, U. Kolb, Ch. Helling, A. Carter, P. Wheatley, A. C. Cameron, B. Loeillet, D. Pollacco, R. Street, H. C. Stempels, E. Simpson, S. Udry, Y. C. Joshi, R. G. West, I. Skillen, and D. Wilson, *Astrophys. J. Lett.* **714**, L222 (2010).
5. J. Llama, K. Wood, M. Jardine, A. A. Vidotto, Ch. Helling, L. Fossati, and C. A. Haswell, *Mon. Not. R. Astron. Soc.* **416**, L41 (2011).
6. A. A. Vidotto, M. Jardine, and Ch. Helling, *Mon. Not. R. Astron. Soc.* **414**, 1573 (2011).
7. D. Bisikalo, P. Kaygorodov, D. Ionov, V. Shematovich, H. Lammer, and L. Fossati, *Astrophys. J.* **764**, 19 (2013).
8. D. V. Bisikalo, P. V. Kaygorodov, D. E. Ionov, and V. I. Shematovich, *Astron. Rep.* **57**, 715 (2013); arXiv:1311.4441v2[astro-ph.EP](2013).
9. E. M. Schneiter, P. F. Velazquez, A. Esquivel, and A. C. Raga, *Astrophys. J. Lett.* **671**, L57 (2007).
10. V. Bourrier and A. Lecavelier des Etangs, *Astron. Astrophys.* **557**, A124 (2013).
11. M. K. Abubekkerov, N. Yu. Gostev, and A. M. Cherepashchuk, *Astron. Rep.* **53**, 722 (2009).
12. M. K. Abubekkerov, N. Yu. Gostev, and A. M. Cherepashchuk, *Astron. Rep.* **54**, 1005 (2010).
13. M. K. Abubekkerov, N. Yu. Gostev, and A. M. Cherepashchuk, *Astron. Rep.* **55**, 1051 (2011).
14. M. K. Abubekkerov and N. Yu. Gostev, *Mon. Not. R. Astron. Soc.* **432**, 2216 (2013).
15. A. Claret, *Astron. Astrophys.* **552**, A16 (2013).
16. H. A. Knutson, D. Charbonneau, R. W. Noyes, T. M. Brown, and R. L. Gilliland, *Astrophys. J.* **655**, 564 (2007).
17. F. Pont, R. L. Gilliland, C. Moutou, D. Charbonneau, F. Bouchy, T. M. Brown, M. Mayor, D. Queloz, N. Santos, and S. Udry, *Astron. Astrophys.* **476**, 1347 (2007).
18. F. Pont, H. Knutson, R. L. Gilliland, C. Moutou, and D. Charbonneau, *Mon. Not. R. Astron. Soc.* **385**, 109 (2008).

*Translated by L. Yungel'son*